Simfit and Focus Diversity: methods for determining the focus of the SIRTF telescope in space without a focus slew

William F. Hoffmann[a], Joseph L. Hora[b], J. Eric Mentzell[c], Catherine T. Marx[c], Peter R. Eisenhardt[d]

[a]Steward Observatory, The University of Arizona, Tucson, AZ 85721
[b]Harvard-Smithsonian Center for Astrophysics, Cambridge, MA 02138
[c]NASA/Goddard Space Flight Center, Greenbelt, MD 20771
[d]Jet Propulsion Laboratory, California Institute of Technology, Pasadena, CA 91109

ABSTRACT

Because of concern over possible failure of the SIRTF cryogenic focus mechanism in space, the SIRTF Project Office has directed that the focus should be set before launch so that the telescope arrives in orbit as close to optimum focus as possible. Then focus evaluation and determination of any required focus change to achieve best focus must be carried out without the conventional approach of a focus slew. For these tasks we have created two methods: Simfit and Focus Diversity. Simfit is a procedure for comparing an observed stellar image with a family of simulated point-source images with a range of focus settings. With a sufficiently accurate as-built telescope model for creating the simulated images, the focus offset and direction can be accurately and unambiguously determined because of the change in image appearance with defocus. Focus diversity takes advantage of the variation of best-focus setting over the instrument's focal plane due to focal plane curvature and tilt and offsets between different instrument channels. By plotting an image quality parameter, such as noise-pixels, for observed stars at several positions on the focal plane versus a defocus variable, the focus error and direction can be determined. We have developed an efficient program for carrying out these procedures. The validity of this program has been successfully confirmed using point-source images observed with three bands of the IRAC camera during a double-pass optical test of SIRTF in a Ball Aerospace cryogenic test chamber. The two procedures are described and are illustrated with these results

Keywords: simfit, focus diversity, telescope focus, simulated images, optical testing, infrared, cryogenic, SIRTF, IRAC

1. INTRODUCTION

SIRTF is the Space Infrared Telescope Facility[1], scheduled for launch on January 9, 2003. The telescope is an 85 cm f/12 Ritchey-Cretien constructed of beryllium. It will have an operating temperature of less than 5.5 K and is specified to be diffraction limited at a wavelength of 6.5 μm. There are three science instruments providing imaging from 3 to 180 μm and spectroscopy from 5 to 40 μm. IRAC (Infrared Array Camera[2]), which operates at the shortest wavelengths and has the highest spatial resolution, has the primary responsibility for telescope image quality and focus evaluation.

IRAC has four arrays sharing the focal plane in pairs. The nearly overlapping pass-bands are centered at 3.56, 5.69, 4.51, and 7.96 μm. Each array has 256 x 256 pixels with a pixel scale of 1.21 arc-seconds. A consequence of this pixel scale is that a point-source image is under-sampled, particularly by channels 1 and 2 for which λ/D equals 0.7 and 0.9 pixels, respectively.

The challenge addressed in this paper is how to use IRAC to determine the departure of the telescope focus from optimum focus with images obtained at just one focus setting, namely the launch setting. To avoid potential risk of failure of the (cryogenic) secondary focus mechanism, the SIRTF Project Office has directed that there be no conventional focus slew to determine best focus. Rather, once the defocus has been determined from images at the initial focus setting, there can be at most one set of moves directly to the optimum focus. To achieve this goal, we have created two methods for focus determination, Simfit and Focus Diversity. The remainder of this paper describes these

two methods and illustrates them with simulated data for SIRTF in space and with observed images during environmental chamber double-pass optics verification tests. For these illustrations we have used IRAC Channel 1. The methods work equally well with the other IRAC channels.

2. SIMFIT

Simfit is a mathematical method for determining the focus setting of a telescope or instrument by comparing an observed image of a source with a set of simulated model images obtained at closely spaced model focus settings. The name stands for fitting one of a set of simulated images to an observed image. This method is useful anytime the focus of the system must be determined without focus slew, focus dither, or step-wise approach to the optimum focus. Creation of a satisfactory set of simulated images is central to the success of the method. We describe the creation of simulated images and the process of Simfit in the context of the SIRTF and IRAC requirements and characteristics.

2.1 Steps for creating the SIRTF/IRAC simulated images

Throughout this discussion and the analysis, we have chosen as the basic focus parameter the telescope secondary focus setting. This is specified in μm of axial motion at the secondary. A positive motion moves the secondary away from the primary and the in-focus image at the SIRTF focal plane toward the secondary. There are three control steps of the focus mechanism stepper motor per μm of motion. The zero of the secondary setting is arbitrary. We have generally set it to be the mean of the best-focus settings for the nine focal plane positions of Channel 1.

Creation of satisfactory simulated images depends critically on an optical model that faithfully represents the system. For SIRTF and IRAC, the model was created in the Optical Research Associates ray-trace program, CodeV. The wavefront deformations, properties, and positions of the optical elements in the model were taken from measurements of individual components and subassemblies obtained at the operating temperatures. The IRAC component properties include variation with wavelength. The model was verified and refined by comparing model images to measured images obtained during end-to-end tests at Ball Aerospace & Technologies Corporation using their largest thermal vacuum chamber, known as the "Brutus" chamber[3]. For this purpose, the model for SIRTF in orbit had to be altered for additional components, with their wavefront deformations where known to be significant. These are changed geometry in the test chamber configuration, a distorted auto-collimation flat, a cryostat window, an extended "point source", and the presence of gravity. Given the model, simulated images are created by ray tracing allowing for varying spectral response and for diffraction. For SIRTF/IRAC, this is done in the following steps.

1. Create a set of rays from a point source at infinity to the focal plane array, uniformly covering the SIRTF aperture and sampling the wavelength range of the array. This is done for a particular telescope secondary focus setting and position on the array. For testing on the ground and measuring the focus in orbit, we have chosen nine “canonical” positions in each field-of-view to provide reasonable spatial sampling. These positions are the center, the four corners, and four additional locations on the array row and column centerlines, 0.6 of the way from the center to the edge.

2. Use the ray-trace data to compute the wavefront aberration of the system. Then by Fast Fourier Transform, compute the diffraction image distribution at the plane of the array for each wavelength sampled.

3. Sum these intensity distributions over wavelength, weighting for the spectral response of the array and filter and for the source spectrum (Rayleigh-Jeans for a star).

4. Bin the summed wavelength intensity data into a grid of sub-pixels each one-fifth the size of an IRAC pixel. This grid is centered on the source and has the same number of sub-pixels as IRAC pixels on the array.

5. Format the results as a FITS image file.

2.2 Simfit concept and approach

Underlying Simfit is the fact that as an instrument or telescope is defocused, the image of a point source not only becomes larger, but also changes its shape due to changing ray paths through the system and the effects of pupil location, obscuration, optical aberrations, and diffraction. These changes are different on the two sides of best focus. This is true even very close to best focus. By comparing an observed image with a family of simulated images and determining which simulated image fits most closely to the observed image, we can uniquely determine the telescope focus setting for the observed image, hence both the distance and director of defocus.

We have used two different algorithms for the image comparison, cross correlation and blink. Cross correlation is a multiplicative comparison. Blink is a subtractive comparison. The name, blink, is derived from the classical method for discerning a small motion or brightness change of a source in a star field by a blink comparator. The algorithms are given in Equations 1 and 2 where *Star* is the observed source, *Simin* is a member of the family of simulated images, and *i* and *j* are indices for the rows and columns of a portion of the array covering the source.

Both algorithms result in a single number for the quality of the fit that is 1 for a perfect fit and 0 for no overlap of the images. Both require that the zero flux level to be accurately established. Both require that the simulated images be precisely registered to the position of the observed image relative to a pixel center. That is, the centroids of the observed and simulated images must be identical. It is desirable that the comparison be carried out over a portion of the array centered on the source and containing at least 90% of the source flux. We have generally used the blink algorithm, which provides greater sensitivity near best focus.

$$Crosscor = \frac{\sum_{i,j} Star_{ij} \times Simim_{ij}}{\sqrt{\left(\sum_{i,j} \left(Star_{ij}\right)^2 \times \sum_{i,j} \left(Simim_{ij}\right)^2\right)}} \tag{1}$$

$$Blink = 1 - 0.5 \times \sum_{i,j} \left| \frac{Star_{ij}}{\sum_{i,j} Star_{ij}} - \frac{Simim_{ij}}{\sum_{i,j} Simim_{ij}} \right| \tag{2}$$

2.3 Steps in the Simfit process

The program which carries out the Simfit calculations from reading observed and simulated image files to displaying graphically and numerically the results is a Mathcad 2001 Professional worksheet. Mathcad provides ample array and imaging processing and image display capability. Its "you see what you get" format is convenient for a non-programmer. The steps in the program are listed below.

1. For a selected IRAC channel, read the file of a star image obtained at one of the nine canonical locations in the array field of view (see Section 2.1, step 1 for definition of these locations).

2. Process the image to set the background flux level to zero.

3. Locate the position of the star by row and column and compute the row and column centroids using a chosen analysis box size.

4. Read the set of sub-pixel simulated image files for the same channel and nearest field location covering a range of telescope focus setting. For SIRTF these are at a 2.5 or 5 μm secondary focus spacing.

5. Blur the simulated images for all channels for telescope jitter and for channels 1 and 2 for charge diffusion, which occurs in the InSb arrays.

6. For each blurred simulated image combine the sub-pixels into IRAC sized pixels over the chosen analysis box size, shifting to provide the same centroid as the star image. The shifting is done to fractional sub-pixels by 16-point bi-quadratic interpolation. The process is iterated until the centroids agree to within 0.01 pixels

7. Carry out the blink (or cross correlation) algorithm between the star and each of the simulated images. The result is a set of values of the Simfit parameter that peaks for the simulated image whose focus is closest to that of the star image.

8. Repeat steps 6 and 7 using a set of simulated images with closer focus spacing obtained by interpolation from the initial set.

9. Interpolate the fine-focus results to obtain the focus setting for the best-fitting image to a fraction of a μm at the secondary.

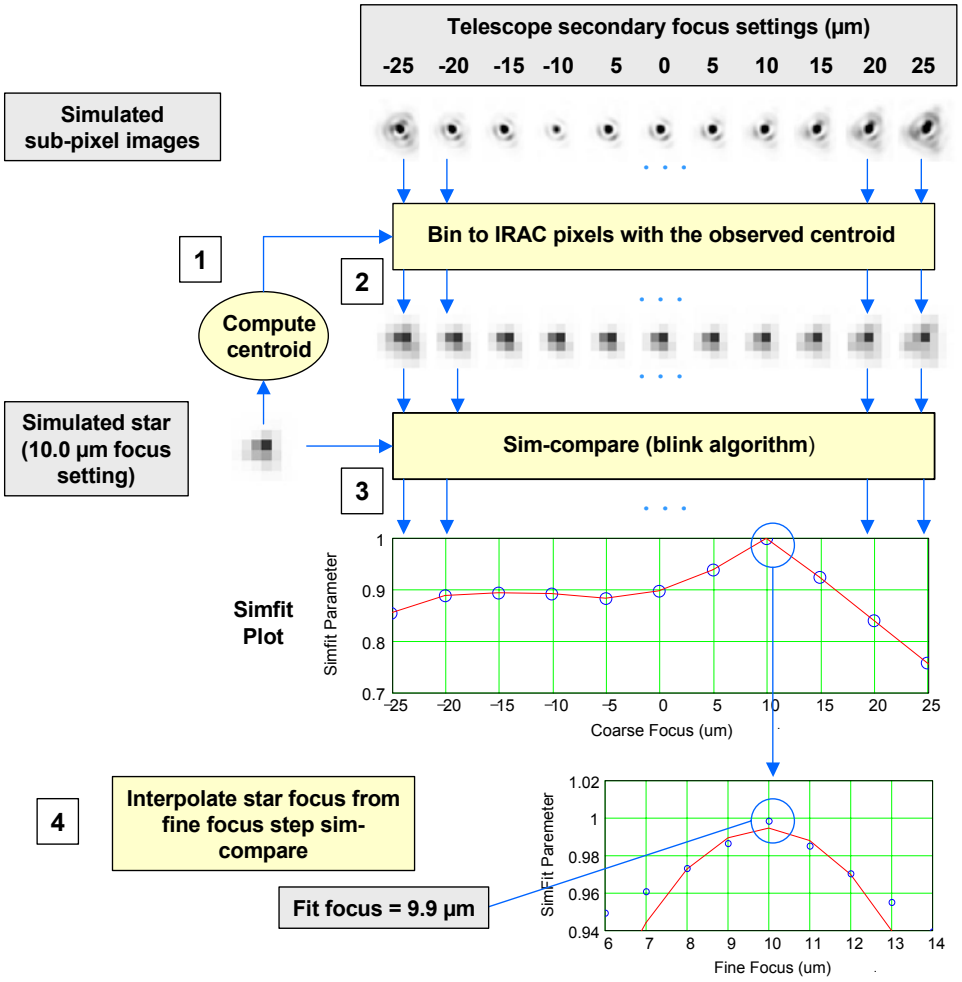

Figure 1. Simfit focus evaluation method with a simulated star. This figure shows an input family of simulated images, a simulated "observed" star, and the four steps required to get from the inputs to the resulting fit focus. The sub-pixel simulated images show diffraction rings and image structure. The binned images show the IRAC Channel 1 under-sampling of the Airy disk with one pixel equaling 0.71 λ/D. The last step achieves an interpolated fit focus of 9.9 μm, very close to the simulated star setting of 10.0 μm.

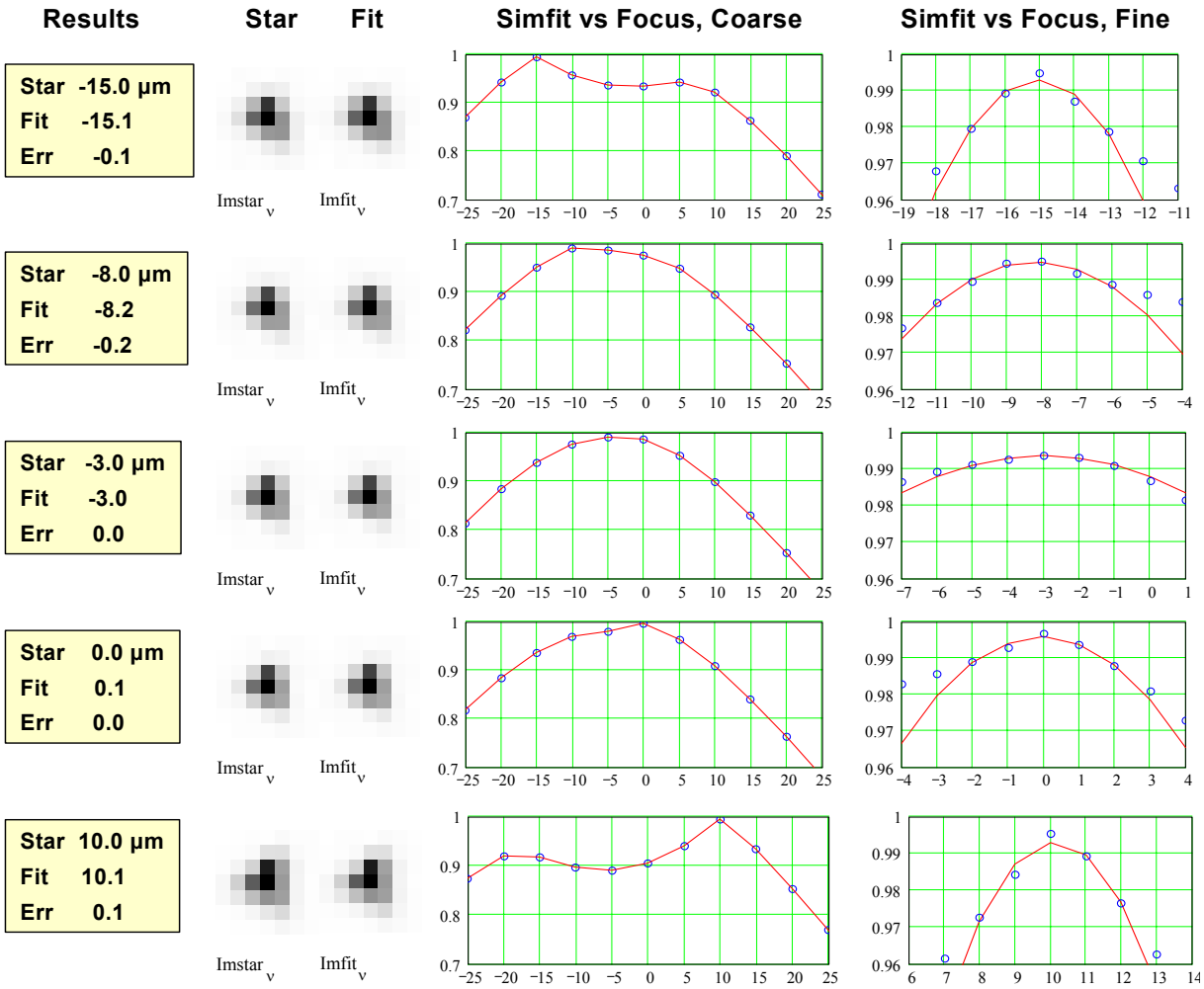

Figure 2. Examples of the results of Simfit for simulated star images for SIRTF and IRAC. The simulations are carried out for Channel 1 center position using the ioc_oct01_rj SIRTF/IRAC model. The simulated "observed" images are calculated for telescope secondary focus settings –15, -8, -3, 0, and 10 µm. For negative focus values, the secondary is closer to the primary. Read, shot, and flat-field noise have been added to the observed images, which are scaled to represent a star with brightness 6th magnitude. The flat field noise is a variation in the sensitivity from one pixel to another. It has been chosen to have a standard deviation of 1%. Both the simulated stars and the comparison simulated images have had the effects of array charge diffusion and predicted telescope jitter added. The focus setting for the simulated star, the Simfit focus, and the error are given in the boxes at the left. The two images are for the simulated star and the Simfit image. The two images are not visually distinguishable, although one has noise and the other does not and their focus settings are slightly different. In the center graph, the circles plot the Simfit parameter versus the focus setting for the family of comparison images. The curve connects the points. The focus values are relative to the model zero value. The graph at the right is the same for finer focus steps. The Simfit focus value is determined from the peak of the parabola best-fitting the center five points on this plot. The -15 and +10 µm center plots show the secondary peak on the opposite side of best-focus from the main peak where the image is similarly blurred from defocus, but has a very different structure. The –3 µm plot is very near best-focus, as indicated by the symmetry of the Simfit curve. The 8 and 0 µm focus plots show that the method clearly distinguishes which side of best-focus the star is when it is near best-focus. The errors are all within +/ 0.2 µm. This is much less than one diffraction focus unit ($[f/]^2 \times \lambda$), which for 3.56 µm wavelength corresponds to a 5.1 µm focus motion at the secondary.

The Simfit process is shown graphically in Figure 1 using the SIRTF/IRAC model (ioc_oct01_rj) for IRAC Channel 1 and a noiseless simulated star. The simulated sub-pixel images show that this model predicts nearly diffraction-limited performance at 3.56 μm, considerably better than the 6.5 μm diffraction limited specification. The simulated star and binned images clearly under-sample the diffraction pattern. However, this under-sampling does not degrade the accuracy of the Simfit process.

2.4 Examples of Simfit results with simulated star images

Figure 2 gives examples of the results of Simfit for simulated star images for SIRTF and IRAC, Channel 1. Five "pseudo star" images are calculated and analyzed for focus settings –15, -8, -3, 0, 10 μm. This figure shows images of the star and fit images and coarse and fine Simfit plots. Noise and detector artifacts have been added to the images. The resulting errors in the focus determination range over +/- 0.2 μm, approximately 1/25 of the diffraction focus unit ($[f/]^2 \times \lambda$) at the wavelength of Channel 1.

3. FOCUS DIVERSITY

Focus diversity is the variation in best-focus setting over the field-of-view of an imaging instrument or from one instrument channel to another. This would normally be considered to be a weakness of the design or assembly of an instrument. However, the presence of focus diversity can be used to accurately determine the focus of a system relative to an optimum focus with images obtained at only one focus setting of the system. This is the same objective as that given for the Simfit method. The procedures and requirements of the two methods are very different. As a consequence, these two methods are complementary and provide an excellent check on each other. Two of the major differences are:

1) Focus Diversity and Simfit both require an optical model, Focus Diversity to establish analysis parameters and Simfit to create simulated images. However Focus Diversity is less affected by model errors than Simfit.
2) Focus Diversity requires a set of images obtained at different positions in the field-of-view or in different instrument channels, whereas Simfit can, in principle, determine the telescope focus from a single star image.

3.1 Noise-pixels as a measure of image defocus

A suitable measure of the effect of defocus on image quality is essential to the focus diversity method. This measure must not be seriously degraded by image under-sampling or noise. For this we have chosen noise-pixels[4]. Noise-pixels are the equivalent number of pixels for calculating the random noise when an image is spatially filtered for optimum faint point-source detection. The optimum filter is directly related to the point-spread-function of the system. The equivalent number of noise pixels is given in Equation 3. *Star* can be the instrument point-spread-function or a high signal-to-noise image of a point source. *i* and *j* are indices for the rows and columns of a portion of the array covering the source. If the star flux is equally distributed over one or more pixels, noise-pixels equal the number of pixels covered by the star. The more concentrated the image of a star, the smaller the number of noise pixels.

$$NoisePixels(Star) = \frac{\left(\sum_{i,j} Star_{ij}\right)^2}{\sum_{i,j}\left(Star_{ij}\right)^2} \tag{3}$$

Noise-pixels are directly related to a number of more familiar concepts. Integration time for faint source detection at a given sensitivity increases linearly with noise-pixels. The sensitivity for a fixed integration time is proportional to the square root of noise-pixels. The inverse of noise-pixels, called "sharpness", is a measure of image concentration. Noise-pixels can be thought of as a measure of the extent, or blur of an image of a point source.

The calculation of noise-pixels is somewhat sensitive to pixel phase (location of source peak or centroid relative to a pixel center). Therefore it is important that the images have the same pixel phase for plotting noise-pixels for different focus settings or focal plane positions. For comparison of noise-pixels from one position to another in the focal plane or

from one IRAC channel to another we use normalized noise-pixels. This is the ratio of the measured noise-pixels to noise-pixels at best focus for that channel and position on the focal plane. This accounts for differences in noise-pixels at best focus over the focal plane and for different channels due to increased image size from diffraction.

3.2 The behavior of noise-pixels with defocus

As with other measures of defocus, such as full-width-half-maximum, when an instrument is scanned over a focus range, noise-pixels for a point source reach a minimum at best focus and increase on either side of best focus. For an image that is structured due to aberrations, the best-focus setting will be slightly different for different measures of image blurring. The best focus determined by noise-pixels gives the best point source signal-to-noise.

Figure 3 shows plots of noise-pixels versus secondary focus setting using IRAC Channel 1 simulated images at three focal plane positions. For each focal plane location, the image quality parameter, noise-pixels, determines a curve that has a minimum at best focus. The curves shown are cubic spline fits to the points and are very nearly the same at each position. We call these curves "defocus curves". The differences in the focus setting for the defocus curves' minima give the variation in best-focus over the IRAC field-of-view. This variation occurs because of a mismatch between the curved focal surface created by the optics and the flat array and by slight tilt alignment errors. In addition, there are offsets in best focus from one channel to the others. These effects are not large enough to cause any problem for the camera meeting its image quality specifications, but they provide the necessary focus diversity for determining the telescope focus setting. The same focus scan method was used during the SIRTF environmental optical tests to obtain measured, as opposed to model, best-focus settings. These plots are used to obtain the three items required for focus diversity analysis: the best-focus settings, noise-pixels at best focus, and the defocus curve.

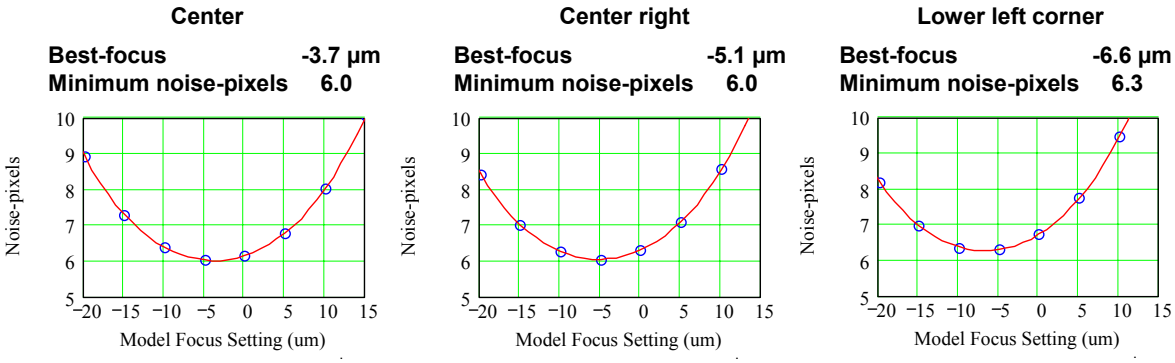

Figure 3. Noise-pixels plotted as a function of secondary focus setting. The noise-pixels are plotted for three positions as indicated on the IRAC Channel 1 focal plane. The circles are noise-pixels calculated with noise-less simulated SIRTF/IRAC images using the ioc_oct01_rj model. The curves are fit to the points with a cubic spline. We call these curves "defocus curves". The best-focus secondary settings for these positions range from –3.7 to –6.6 µm relative to the model zero setting. This is due to field curvature and tilt. These plots provide the three items needed for each position for focus diversity analysis: best-focus setting, minimum noise pixels at best focus, and defocus curve.

3.3 Focus Diversity concept and approach

The knowledge of the relative secondary setting for best-focus over the field of an IRAC channel, as illustrated in Figure 3, is an essential part of the focus diversity concept. As the telescope focus is changed, the normalized noise-pixel values follow along a defocus curve that has a different minimum location for each position. Figure 4 illustrates this for one focus setting, -15.0 µm, for three focal plane positions. The left-hand plot shows the -15.0 µm normalized noise-pixels points with their individual defocus curves. The right hand plot shows the points versus defocus as defined in Equation 4 and illustrated for the center position in Equation 5. In this plot the three defocus curves fall on top of each other and are centered at zero defocus. The three points fall nicely on the combined curve.

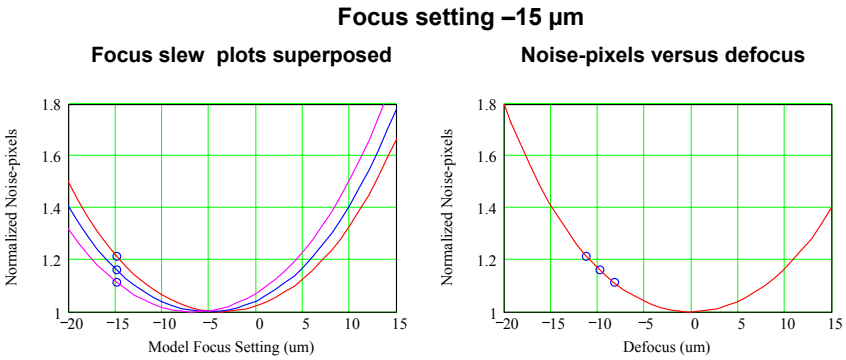

Figure 4. Normalized noise-pixels for IRAC Channel 1 for three focal plane positions at a focus setting of -15 µm. The left plot provides a superposition of the -15 µm points and the defocus curves for the three positions, all plotted versus the secondary focus setting. The plot at the right gives the same data plotted versus the defocus variable defined in Equation 4 and illustrated in Equation 5. In this plot, the three defocus curves fall on top of each other and the three points fall nicely on the combined defocus curve.

$$Defocus = FocusSetting - Bestfocus \tag{4}$$

$$-11.3 \quad = \quad -15 \quad - \quad -3.7 \tag{5}$$

In principle, measurement of the noise-pixels at just one location in the focal plane can be used to uniquely determine two possible focus settings, one on each side of best focus for that location. Adding a measurement of noise-pixels at a second location removes this ambiguity. Measurement of noise-pixels at several locations permits best fitting to determine both the focus setting and a correction to the model minimum noise pixel value.

The steps for Focus Diversity are given in Figure 5. This figure shows as inputs, cropped images for nine positions on the focal plane of IRAC Channel 1, the best-focus setting and minimum noise-pixels for each position, and the defocus curve used in the plots. The steps are to calculate noise pixels, calculate the defocus variable for each position for a given focus setting, and plot the normalized noise pixels versus defocus. In Figure 5, the latter two steps are carried out first with a focus setting of zero, to illustrate the procedure. For this focus setting, the points clearly do not lie on the line, since zero is far from the –15 µm setting for the simulated stars. The second and third steps are then repeated with the focus setting determined by a least-square fit of the points to the defocus curve. The fitting procedure also allows for a small correction to the minimum noise pixels to correct for any error in determining this parameter from the model. The point given by the square is for the center position, which for this focus setting is the furthest from best focus and hence has the largest noise-pixels.

3.4 Examples of Focus Diversity results with simulated star images

Figure 6 gives examples of the results of Focus Diversity for simulated star images for SIRTF and IRAC, Channel 1. Five sets of nine "pseudo star" images are calculated and analyzed for focus settings -15, -8, -3, 0, and 10 µm. These are the same five focus settings used with Simfit analysis in Figure 2. Figure 6 shows plots of the normalized noise-pixels and defocus curve versus defocus and the resulting fit focus settings. Also shown are three-dimensional bar graphs of the normalized noise pixels for each focal plane position. These show clearly the mismatch of the curved focal plane to the flat detector and the change in direction of curvature on the two sides of best-focus. Noise and detector artifacts have been added to the images. The resulting errors in the focus determination range over +/- 0.5 µm, approximately 1/10 of the diffraction focus unit at the wavelength of Channel 1.

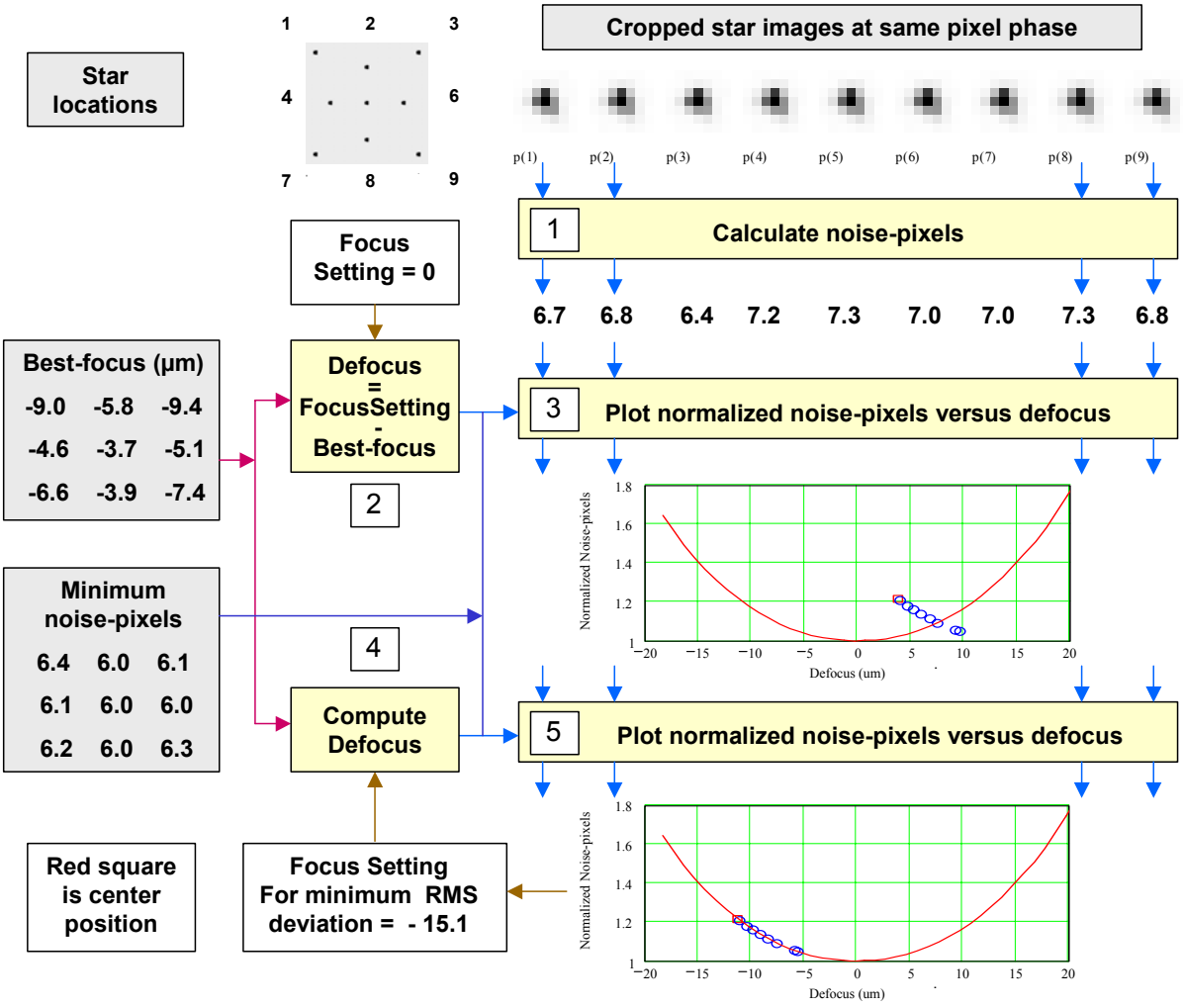

Figure 5. Focus Diversity method with nine simulated stars, Channel 1, at a focus setting of -15 µm. The inputs to the focus diversity method are the cropped images of stars at a set of focal plane positions, the best focus secondary settings and minimum noise-pixels for the same positions, and the defocus curve appropriate for the same positions. The stars should be observed at nearly the same pixel phase to avoid scatter due to the variation of noise-pixels with pixel phase. The first three steps shown are to calculate noise-pixels, to calculate the defocus variable from an arbitrary focus setting (zero) and best-focus and to plot normalized noise pixels versus defocus. Steps 4 and 5 repeat the previous two steps, this time calculating a focus setting that minimizes the RMS deviation of the normalized noise-pixels from the defocus curve. In this example, the resulting focus setting is -15.1, very close to the -15.0 setting for the simulated star.

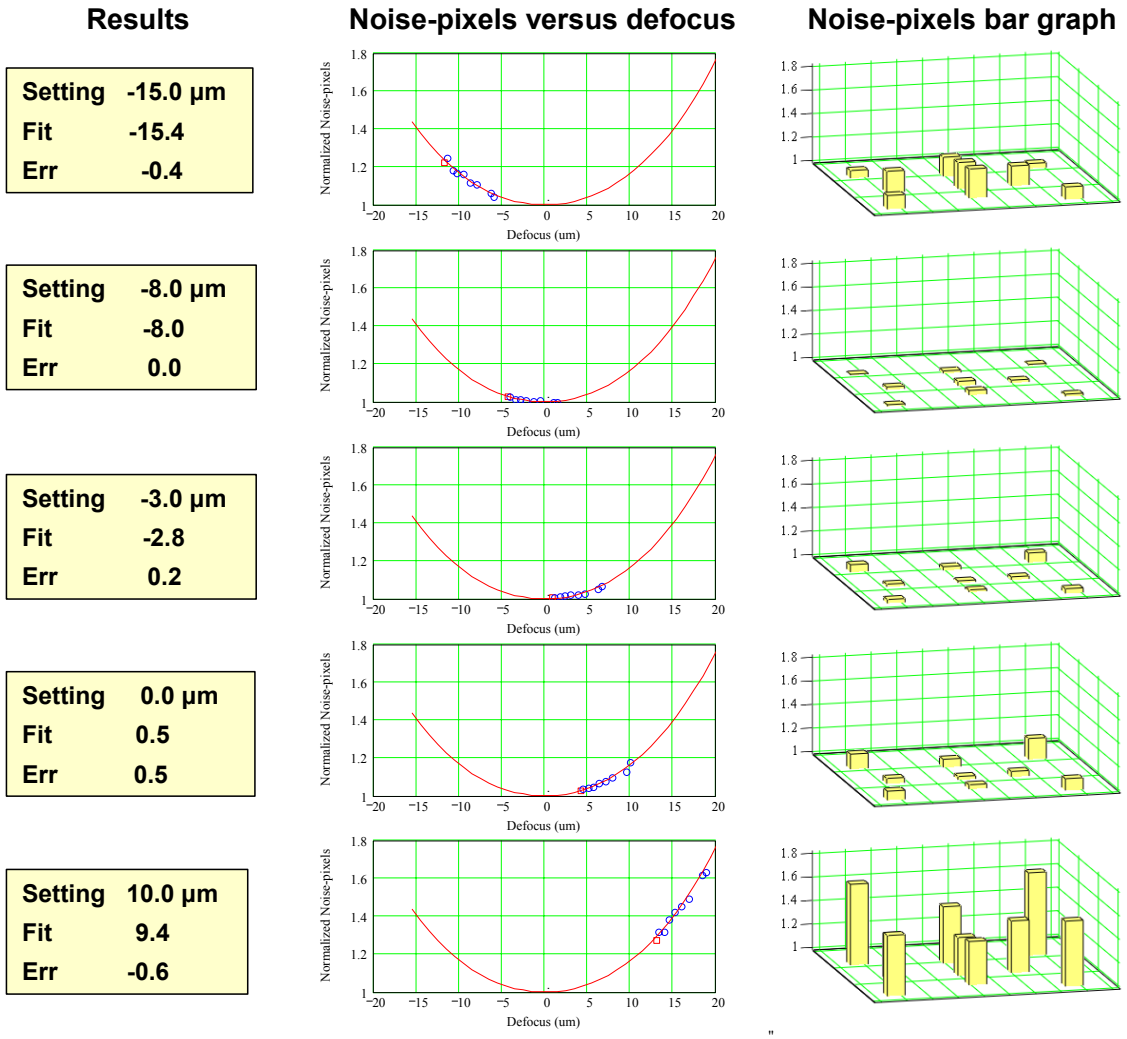

Figure 6. Focus Diversity results from SIRTF and IRAC Channel 1 simulations at nine focal plane positions. The simulations are carried out for Channel 1 using the ioc_oct01_rj SIRTF/IRAC model. The simulated "observed" images are calculated for telescope secondary focus settings –15, -8, -3, 0, and 10 µm. For negative focus values, the secondary is closer to the primary. Read, shot, and flat-field noise have been added to the observed images, which are scaled to represent a star with brightness 6th magnitude. The flat field noise is a variation in the sensitivity from one pixel to another. It has been chosen to have a standard deviation of 1%. Both the simulated stars and the simulated images have had the effects of array charge diffusion and predicted telescope jitter added. The focus setting for the simulated star, the focus diversity fit, and the error are given in the boxes at the left. In the center graph, the circles plot the normalized noise-pixels for the nine focal plane positions versus the defocus variable calculated for the best fit of the points to the defocus curve. The focus values are relative to the model zero value. The bar graph at the right shows the normalized noise-pixels for the nine focal plane positions. For the negative focus settings (secondary moved toward the primary) the center position on the array is furthest from best-focus resulting in the largest normalized noise-pixels. For positive focus settings, the opposite is true. The fit focus errors are within +/ 0.5 µm, a factor of 10 less than one diffraction focus unit at 3.56 µm.

4. EXAMPLES FROM THE BRUTUS CHAMBER OPTICAL TESTS

An end-to-end optical test of the telescope and instruments was carried out at Ball Aerospace & Technologies Corporation in their large vacuum cryogenic chamber, called the Brutus chamber. The test setup and many of the results are described in detail by Schwenker, *et. al*[5]. The optical tests were carried out double-pass (auto-collimation) with the telescope and flat close to the temperature expected in orbit. This setup had a number of differences from the orbit configuration, requiring a very different optical model as indicated in Section 2.1. Among these differences were the auto-collimation flat, which became distorted at low temperatures, a cryostat window which transmitted at relatively short wavelengths, permitting infrared imaging tests only of IRAC channels 1-3 and the IRS spectrometer shortest

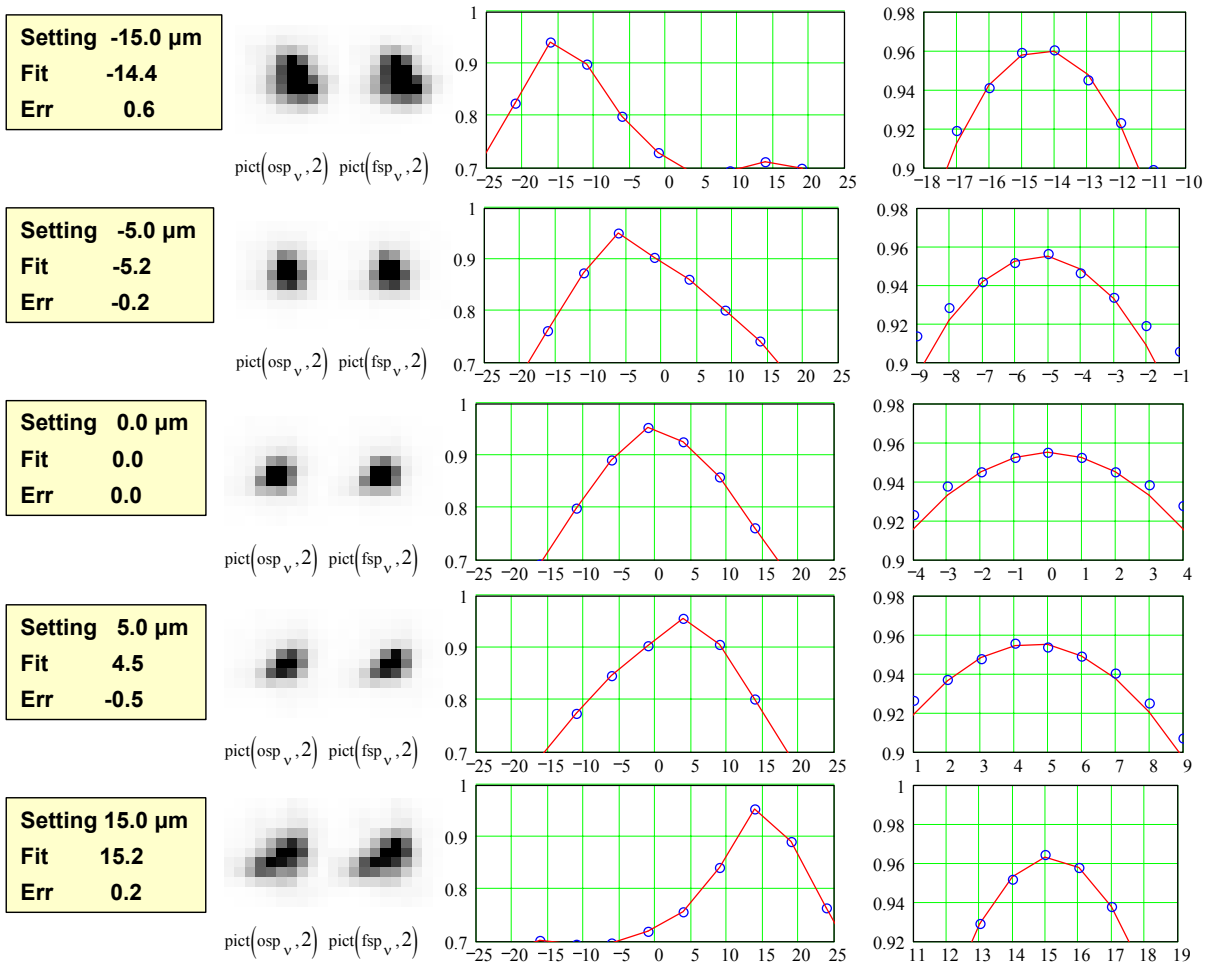

Figure 7. Simfit results from SIRTF and IRAC environmental chamber double-pass measurements. These measurements were carried out at Ball Aerospace & Technologies Corporation in a double-pass (auto-collimation configuration. An "as-built" optical model was created to allow for the double-pass, a distorted auto-collimation flat, a cryostat window, an extended point source, and gravity deformation (swir_br_oct01) and a second model (swir_br_oct01_pm) corrected for phase retrieval measurements. The highest Simfit parameter was obtained with a linear interpolation between models with the phase retrieval model weighted 0.75 and the as-built model 0.25. This mixture was used in the above analysis. The double-pass produces twice the sensitivity of defocus to secondary motion. That and the added aberrations result in much larger images than expected in orbit. Still, the overall accuracy of the analysis is excellent with errors ranging over +/- 0.5 µm.

wavelength channel, an extended "point-source" located off-axis and displaced from the SIRT focal plane, and gravity. The displaced source was brought to focus at the instruments by a large offset of the secondary focus mechanism. The image of the source was placed at the required positions of the instruments' field-of-view by fine tilting of the auto-collimation flat. Figures 7 and 8 illustrate both Simfit and Focus Diversity with real data for IRAC Channel 1. The illustration for Simfit covers secondary focus settings, -15, -5, 0, 5, and 15 µm. The illustration for Focus Diversity covers settings -15, -10, -5, 10, and 15 µm. For the analysis, the model zero was adjusted to agree with the secondary mechanism zero. Two models were available for the analysis, an "as built" model allowing for all the items in the test configuration as measured at operating temperature (swir_br_oct01) and a version of that model corrected for the results of phase retrieval measurements (swir_br_oct01_pm). A linear combination of these models with the first weighted 0.25 and second 0.75 gave the highest Simfit parameter and was used for the analysis for both methods.

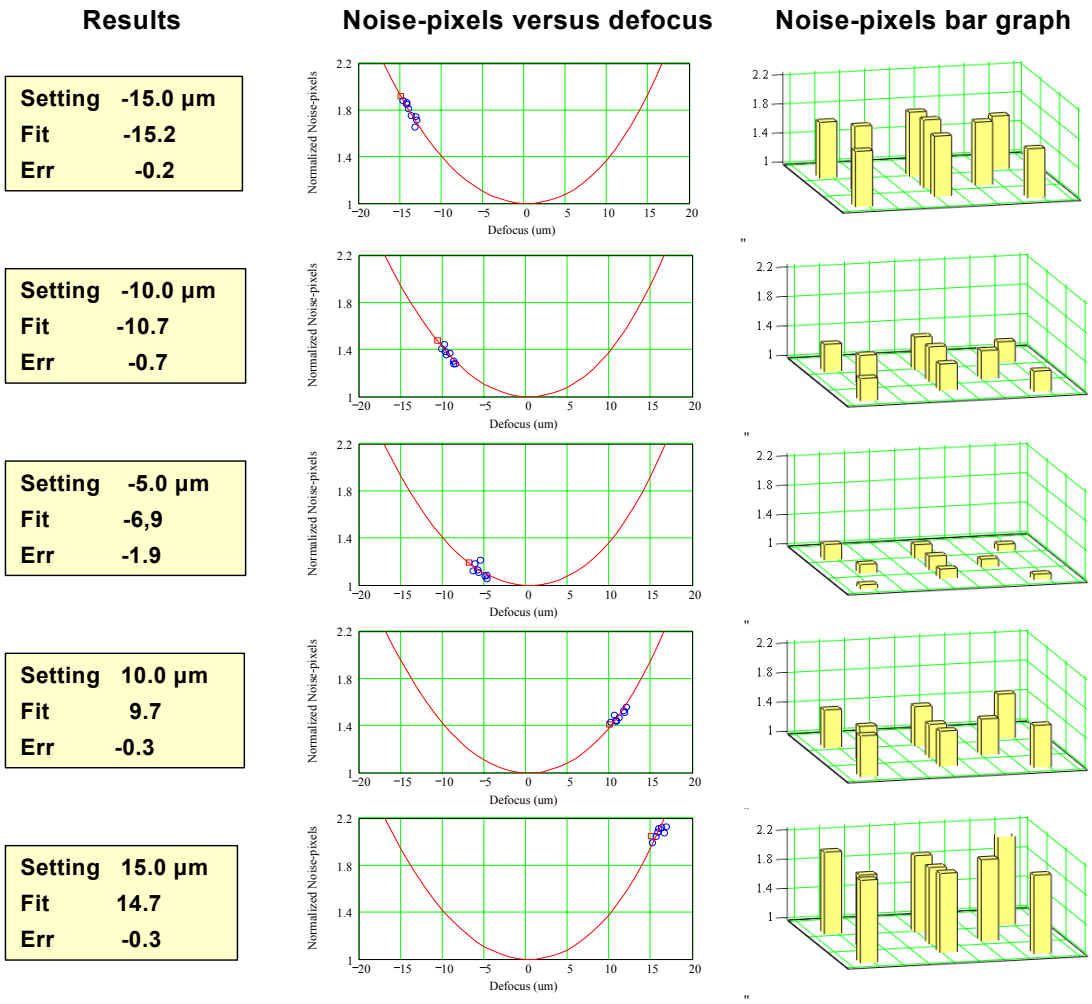

Figure 8. Focus Diversity results from SIRTF and IRAC, environmental chamber double-pass measurements. These measurements were carried out at Ball Aerospace & Technologies Corporation in a double-pass (auto-collimation) configuration using the same model as the Simfit analysis. There was no effort during data taking to obtain images at the same pixel phase. The scatter in the normalized noise-pixel values is largely due to the variation of pixel phase from one position to another. This results in increased error for the focus fit, particularly near best-focus. The error range at large offsets from best-focus is +/- 0.5 µm. For settings near best-focus, the error is 2 µm or larger. In orbit we will obtain dithered images to obtain near zero pixel phase by selection or extrapolation.

Figure 7 shows the results of Simfit analysis. The boxes on the left in this figure give the focus setting, the fit focus determination, and the error. The images in the center are the observed image on the left and the simulated fit image on the right. Differences between the images cannot be easily seen, although they do appear in image subtraction. The two plots give the coarse and fine Simfit plots. The errors for these analyses range over +/- 0.5 μm, which is exceedingly good and a testimony to the quality of the combined model. Using either of the models alone result in larger, but still satisfactory, errors.

Figure 8 shows the results of Focus Diversity analysis. The boxes on the left give the same information given in Figure 7. The plots in the center give the defocus curves and the normalized noise-pixels for the nine focal plane positions, both plotted versus defocus. The focus setting in the defocus variable is determined by fitting the points to the curve with minimum RMS deviation. The scatter in the points is large because of the lack of any effort to locate the images for each position to the same pixel phase. The three-dimensional bar plots at the right show the normalized noise-pixels for the nine positions on the focal plane. These show nicely the focal plane curvature that is concave toward the secondary. Negative focus settings move the secondary toward the primary and the focal plane away from the secondary, resulting in greater defocus at the center of the field.

5. SUMMARY

We have created two new methods for determining the focus setting for an optical system without a focus slew, Simfit and Focus Diversity. Simfit determines the focus by comparing an observed image with a family of simulated images covering a range of focus settings. Focus Diversity relies on variation of defocus over the field-of-view of an instrument to determine the overall size and direction of defocus. Both methods depend on an optical model of the system. Simfit is most sensitive to model error, Focus Diversity to random noise. A mathematical program to carry out these procedures has been developed as a Mathcad 2001 worksheet. This has been extensively tested with simulated images for SIRTF/IRAC in space and confirmed with real images obtained with a double-pass configuration in an environmental chamber test. In both the simulations and the test chamber, the two methods generally have errors less than +/- 0.1 times a diffraction focus unit. After the launch of SIRTF, scheduled for January 2003, the two methods will be used to determine defocus and to confirm any refocus, if it is carried out.

6. ACKNOWLEDGEMENTS

We acknowledge funding from NASA Office of Space Science for much of this work. We thank Ed Romana, Robert Gehrz and other members of the SIRTF "Focus Integrated Products Team" for their encouragement and criticism, and John Schwenker and Bill Burmester and others at Ball Aerospace for their suggestions and help, particularly with the image measurements during the Brutus environmental tests.

7. REFERENCES

1. J. L. Fanson, G. G. Fazio, J. R. Houck, T. Kelly, G. H. Rieke, D. J. Tenerelli, M. Whitten, "Space Infrared Telescope Facility (SIRTF)", *SPIE Proceedings* **3356**, pp 478-491, 1998
2. G. G. Fazio, J. L. Hora, S. P. Willner, J. R. Stauffer, M. L. N. Ashby, Z. Wang, E. V. Tollestrup, J. Pipher, W. Forrest, C. McCreight, S. H. Moseley, W. F. Hoffmann, P. Eisenhardt, & E. L. Wright, "The Infrared Array Camera (IRAC) for the Space Infrared Telescope Facility (SIRTF)", *SPIE Proceedings,* **3354**, pp. 1024-1031, 1998.
3. J. P. Schwenker, B. R. Brandl, W. L. Burmester, J. L. Hora, A. K. Mainzer, P. C. Quigley, J. E. VanCleve "SIRTF-CTA Optical Performance Test", *SPIE Proceedings*, [4850-48]**,** 2002
4. E. L. Wright, "On using a space telescope to detect faint galaxies", *PASP*, **97**, pp 451-453, 1985
5. J. P. Schwenker, B. R. Brandl, W. F. Hoffmann, J. L. Hora, A. K. Mainzer, J. E. Mentzell, J. E. VanCleve, "SIRTF-CTA Optical Performance Test Results", *SPIE Proceedings*, [4850-05], 2002